

# Image Hallucination with Feature Enhancement

Zhiwei Xiong\*  
University of Science and Technology of China  
Hefei 230027, China  
xzw@mail.ustc.edu.cn

Xiaoyan Sun, Feng Wu  
Microsoft Research Asia  
Beijing, 100190, China  
{xysun, fengwu}@microsoft.com

## Abstract

Example-based super-resolution recovers missing high frequencies in a magnified image by learning the correspondence between co-occurrence examples at two different resolution levels. As high-resolution examples usually contain more details and are of higher dimensionality in comparison with low-resolution ones, the mapping from low-resolution to high-resolution is an ill-posed problem. Rather than imposing more complicated mapping constraints, we propose to improve the mapping accuracy by enhancing low-resolution examples in terms of mapped features, e.g., derivatives and primitives. A feature enhancement method is presented through a combination of interpolation with prefiltering and non-blind sparse prior deblurring. By enhancing low-resolution examples, unique feature information carried by high-resolution examples is decreased. This regularization reduces the intrinsic dimensionality disparity between two different resolution examples and thus improves the feature mapping accuracy. Experiments demonstrate our super-resolution scheme with feature enhancement produces high quality results both perceptually and quantitatively.

## 1. Introduction

Example-based super-resolution, also known as image hallucination, has become a hot research topic since it was first proposed by Freeman et al. in [1]. Different from conventional super-resolution that combines multiple low-resolution (LR) images to form a high-resolution (HR) one, image hallucination generates an HR image from a unique LR source, with the help of a database consisting of co-occurrence examples at two different resolution levels. Examples extracted from image patches present visually salient features, e.g., derivatives and primitives. Usually, LR features are obtained from downsampled images while HR features from the difference images lost during down-sampling, so the sum of total feature energy is conserved. In hallucination, the missing HR features are deduced from

\*This work was done during Z. Xiong's internship at MSRA.



Figure 1: The “Monarch” image at 3× magnification. Left: practical hallucination [2]. Right: anchor hallucination.

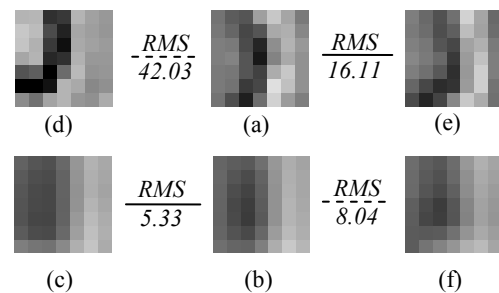


Figure 2: A typical inaccurate LR-HR feature mapping. (a) real missing HR feature patch; (b) input LR feature patch corresponding to (a); (c) NN matching of (b) in the database; (d) HR feature patch corresponding to (c); (e) NN matching of (a) in the database; (f) LR feature patch corresponding to (e). Note that (e) is the required result, but it cannot be found since (c) is closer to (b) than (f).

the remaining LR ones through feature mapping.

There are two fundamental problems in hallucination. One is how many examples are sufficient for generic images. Freeman et al. model the relationship between high frequency components at two different resolution levels using a Markov network solved by belief propagation [1]. They have demonstrated that, with a relatively small number of examples, hallucination greatly outperforms functional interpolation. In [2] Sun et al. propose to learn primal sketch priors for hallucination, as the primitive manifold with intrinsic low dimensionality can be more effectively represented by examples. Later, locally linear embedding (LLE) and compressed sensing (CS) are applied

into hallucination [3, 4], where an HR feature is recovered through a combination of certain candidates in the database. These methods greatly extend the generation ability of examples. However, one question arises here if examples in the database are fully exploited? Figure 1 shows a comparison result between practical hallucination [2] and *anchor hallucination*, i.e., using the real missing HR features which are actually unavailable to find their nearest neighbor (NN) matching in the database (consisting of  $10^5$  pairs of examples). The gap in terms of both the perceptual and quantitative quality indicates the best candidates in the database are not found yet in practical hallucination.

The above experiment reveals the second problem in hallucination. How accurate can the LR-HR feature mapping be? In theory, it is an ill-posed problem, as features that can be separated in a high dimensional space are probably not distinguishable in a low dimensional one. Figure 2 shows a typical case that the missing HR feature (more accurately, a candidate close enough to it) does exist in the database, but there are other candidates generating more similar LR features to the input one. In this case, neither NN matching nor combinations over certain supports from the database give the required result. Neighborhood compatibility may be considered as a constraint, but usually is too weak to effectively improve the mapping accuracy. Another possible approach is to strengthen the correspondence between LR and HR features. Ma et al. propose a three-tiered network model for hallucination in [5], where the HR features found in the first round of LR-HR mapping are combined with enhanced LR features and then used in the second round of HR-HR mapping. Though some irregularities introduced by inaccurate feature mapping are removed, this method does not take into account how feature information is lost. So the “enhanced” features may be unreliable or even misleading hallucination.

In this paper, we analyze the feature information loss in the two degradation processes of downsampling; blurring and decimation. Blurring (mostly Gaussian) causes high frequency truncation and decimation leads to spectrum aliasing. Moreover, these two aspects of information loss are dependent on each other. To achieve a reliable feature enhancement, we propose a combination of interpolation with prefiltering followed by non-blind sparse prior deblurring. Prefiltering helps suppress aliased frequency components while deblurring restores some missing high frequency components. As the existent LR feature information is enhanced, the HR feature information to be learned in hallucination is decreased due to feature energy conservation. Also, feature enhancement is applied in preparing the examples. Consequently, the intrinsic dimensionality disparity between LR and HR features is reduced, which improves the feature mapping accuracy in a new perspective. Despite the fact that various methods can further extend the generation ability of examples, we then use the

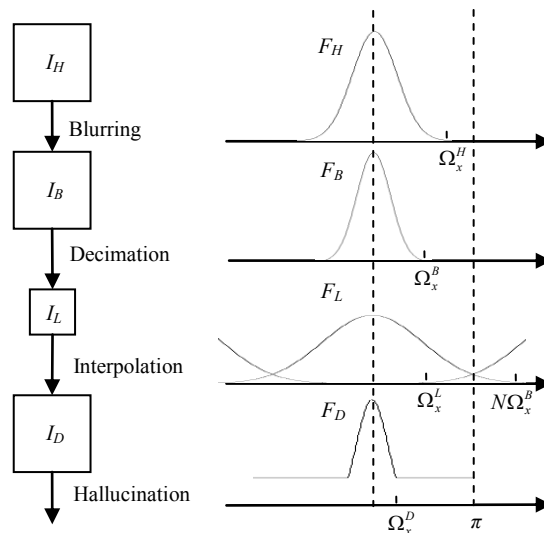


Figure 3: Feature information loss in downsampling. Left: image operations. Right: spectral change in a feature patch. A 1-D spectrum is taken for example.

simplest NN matching and neighborhood averaging to validate the potential of our feature enhancement method in a designed hallucination scheme.

The rest of this paper is organized as follows. In Section 2, we introduce the feature enhancement method based on the analysis of spectral energy loss during downsampling. Section 3 presents our hallucination scheme with feature enhancement. Experimental results are shown in Section 4, and Section 5 concludes this paper.

## 2. Feature enhancement

### 2.1. Information loss in downsampling

We track the feature information loss in downsampling from the spectral energy point of view, as illustrated in Figure 3. Since features are usually related to image derivatives, they can be represented by one or a linear combination of anisotropic Gaussian distributions in a local region. Without loss of generality, we model a feature patch from an original HR image  $I_H$  as

$$f_H = A \exp\left\{-\frac{1}{2} \mathbf{x}^T \mathbf{\Phi}^T \mathbf{\Sigma}^{-1} \mathbf{\Phi} \mathbf{x}\right\}, \quad \text{where} \quad (1)$$

$$\mathbf{\Sigma} = \begin{pmatrix} \sigma_a^2 & 0 \\ 0 & \sigma_b^2 \end{pmatrix}, \quad \mathbf{\Phi} = \begin{pmatrix} \cos \varphi & \sin \varphi \\ -\sin \varphi & \cos \varphi \end{pmatrix}^T, \quad \mathbf{x} = (x, y)^T$$

and  $0 < \sigma_a \leq \sigma_b$ .  $A$  is a magnitude constant. Contours of equal feature value form ellipses and the angle  $\varphi$  denotes the orientation of the minor axis. The length of the minor axis and that of the major axis are proportional to the standard variance  $\sigma_a$  and  $\sigma_b$ , respectively, which reflects the sharpness and density of the intensity transition along these two axes. The major axis is aligned to the direction with

minimum intensity transition in the feature patch, i.e., along the edge orientation.

In the frequency domain, the feature model becomes

$$F_H = A' \exp\left\{-\frac{1}{2} \boldsymbol{\omega}^T \boldsymbol{\Phi}^T \boldsymbol{\Sigma} \boldsymbol{\Phi} \boldsymbol{\omega}\right\}, \quad \text{where} \quad (2)$$

$$A' = 2\pi A \sigma_a \sigma_b, \quad \boldsymbol{\omega} = (\omega_x, \omega_y)^T$$

The original image  $I_H$  is usually downsampled following two steps; blurring and decimation, which first result in a blurred image  $I_B$  and then an LR image  $I_L$ . Blurring is performed to filter out certain high frequency components in  $I_H$  to alleviate spectrum aliasing during decimation, and the commonly used blur kernel is isotropic Gaussian. Consequently, the feature patch from  $I_B$  can be expressed as

$$F_B = A' \exp\left\{-\frac{1}{2} \boldsymbol{\omega}^T \boldsymbol{\Phi}^T \boldsymbol{\Gamma} \boldsymbol{\Phi} \boldsymbol{\omega}\right\}, \quad \text{where} \quad (3)$$

$$\boldsymbol{\Gamma} = \begin{pmatrix} \sigma_a^2 + \sigma_c^2 & 0 \\ 0 & \sigma_b^2 + \sigma_c^2 \end{pmatrix}$$

and  $\sigma_c$  is the standard variance of the Gaussian blur kernel.

Suppose the effective cut-off frequencies in  $F_H$  are  $(\Omega_x^H, \Omega_y^H)$ , and they reduce to  $(\Omega_x^B, \Omega_y^B)$  in  $F_B$ . The spectral energy loss caused by blurring can be calculated as

$$\begin{aligned} \Delta E_B &= E_H - E_B \\ &= \int_{-\Omega_y^H}^{\Omega_y^H} \int_{-\Omega_x^H}^{\Omega_x^H} |F_H|^2 d\omega_x d\omega_y - \int_{-\Omega_y^B}^{\Omega_y^B} \int_{-\Omega_x^B}^{\Omega_x^B} |F_B|^2 d\omega_x d\omega_y \\ &= A'^2 \pi \left( \frac{1}{\sigma_a \sigma_b} - \frac{1}{\sqrt{(\sigma_a^2 + \sigma_c^2)(\sigma_b^2 + \sigma_c^2)}} \right) \end{aligned} \quad (4)$$

One can observe  $\Delta E_B$  increases with the blurring scale  $\sigma_c$ .

Decimation expands the spectrum and causes aliasing. The feature patch from  $I_L$  can be described as

$$F_L = \begin{cases} \frac{A'}{N^2} \exp\left\{-\frac{1}{2N^2} \boldsymbol{\omega}^T \boldsymbol{\Phi}^T \boldsymbol{\Gamma} \boldsymbol{\Phi} \boldsymbol{\omega}\right\}, & |\omega_x| < \Omega_x^L \\ & |\omega_y| < \Omega_y^L \\ \text{aliased,} & \text{otherwise} \end{cases} \quad (5)$$

$$\text{where } \Omega_x^L = 2\pi - N\Omega_x^B, \quad \Omega_y^L = 2\pi - N\Omega_y^B$$

and  $N$  is the decimation factor. Note that aliasing will not happen only if  $\Omega_x^B, \Omega_y^B < \pi/N$ .

Before hallucination, the LR image  $I_L$  is first interpolated to an intermediate HR image  $I_D$ . An ideal interpolation shrinks the spectrum and adapts the feature patch to

$$F_D = \begin{cases} A' \exp\left\{-\frac{1}{2} \boldsymbol{\omega}^T \boldsymbol{\Phi}^T \boldsymbol{\Gamma} \boldsymbol{\Phi} \boldsymbol{\omega}\right\}, & |\omega_x| < \Omega_x^D \\ & |\omega_y| < \Omega_y^D \\ \text{aliased,} & \text{otherwise} \end{cases} \quad (6)$$

$$\text{where } \Omega_x^D = \frac{2\pi}{N} - \Omega_x^B, \quad \Omega_y^D = \frac{2\pi}{N} - \Omega_y^B$$

The spectral energy loss caused by decimation is

$$\begin{aligned} \Delta E_D &= E_B - E_D \\ &= \int_{-\Omega_y^B}^{\Omega_y^B} \int_{-\Omega_x^B}^{\Omega_x^B} |F_B|^2 d\omega_x d\omega_y - \int_{-\Omega_y^D}^{\Omega_y^D} \int_{-\Omega_x^D}^{\Omega_x^D} |F_D|^2 d\omega_x d\omega_y \\ &= 2 \int_{\frac{2\pi}{N} - \Omega_y^B}^{\Omega_y^B} \int_{\frac{2\pi}{N} - \Omega_x^B}^{\Omega_x^B} |F_B|^2 d\omega_x d\omega_y \end{aligned} \quad (7)$$

Since the function inside the integral is always positive,  $\Delta E_D$  increases with the decimation factor  $N$ . Finally, the total spectral energy loss during downsampling is

$$\Delta E = \Delta E_B + \Delta E_D = E_H - E_D \quad (8)$$

$\Delta E$  corresponds to the lost information contained in the HR features, and  $E_D$  to that left in the LR features.

In hallucination, example learning aims to capture the correspondence between feature information at two different resolution levels. However, as the blurring scale and decimation factor increase, the learning performance is often restricted by the fact that the existent LR features hold little information, which greatly degrades the feature mapping accuracy. Therefore, if we can reliably enhance the LR features, i.e., restore part of the lost information first, the mapping process could be improved.

## 2.2. Deblurring with a sparse prior

The two aspects of feature information loss during downsampling are dependent on each other. For a given  $\Delta E$ , increasing  $\Delta E_B$  will decrease  $\Delta E_D$ , and vice versa. We first consider a simple case that  $\Delta E$  mainly comes from blurring. Since the blur kernel is known, one approach for reliable feature enhancement is non-blind deblurring. The relationship between the original image  $I_H$  and the interpolated image  $I_D$  can be represented by

$$I_D = I_H * G + \nu \quad (9)$$

where  $G$  is a Gaussian blur kernel, and  $\nu$  stands for an additive noise, assumed to be a zero-mean and white Gaussian random vector. Generally, deblurring aims to find the MAP estimate of  $I_H$  as

$$I_H^* = \arg \max_{I_H} p(I_H | I_D) = \arg \max_{I_H} p(I_D | I_H) p(I_H) \quad (10)$$

Based on the Gaussian property of the noise, we have

$$p(I_D | I_H) \propto \exp\{-\|I_D - I_H * G\|_2^2\} \quad (11)$$

where  $\|x\|_n$  denotes the  $L_n$ -norm of  $x$ . In order to solve for  $I_H^*$ , an image prior  $p(I_H)$  is required. Here we use a sparse derivative prior as suggested in [7]

$$p(I_H) \propto \exp\{-\|D_h I_H\|_a^a + \|D_v I_H\|_a^a\} \quad (12)$$

where  $a < 1$ ,  $D_h$  and  $D_v$  extract the horizontal and vertical derivatives. Then, the deblurring problem turns into

$$I_H^* = \arg \min_{I_H} \{-\|I_D - I_H * G\|_2^2 + \|D_h I_H\|_a^a + \|D_v I_H\|_a^a\} \quad (13)$$

For the feature patch, (13) equals to

$$\min \{ \|f_H\|_a^a \} \quad \text{s.t.} \quad \|f_H\|_1 = \text{const} \quad (14)$$

According to the feature model in (1), we have

$$\|f_H\|_n^n = \frac{2\pi}{n} A^n \sigma, \quad \text{where} \quad \sigma = \sigma_a \sigma_b > 0 \quad (15)$$

Therefore,

$$\|f_H\|_1 = 2\pi A \sigma = 2\pi C, \quad \text{where} \quad C = \text{const} \quad (16)$$

and then

$$\|f_H\|_a^a = \frac{2\pi}{a} C^a \sigma^{1-a} \quad (17)$$

Since  $\|f_H\|_a^a$  increases with  $\sigma$  given  $\sigma > 0$  and  $a < 1$ , the adopted sparse prior favors a small  $\sigma$  and thus a large  $A$ . In other words, sharp and dense intensity transition is preferred in enhancing the feature patch, which is the desired property for the original HR image. The optimization problem in (13) is solved through an iterative reweighted least squares process [8].

### 2.3. Quadrature prefiltering for antialiasing

As the decimation factor increases, aliasing tends to be severe if the blurring scale is fixed. In the spatial domain, it is the well-known ‘‘jaggy’’ artifacts after interpolation. In conventional hallucination schemes, this is not considered a big issue, as the LR features are weak and the final result mainly depends on the learned HR features. However, since our feature enhancement requires deblurring after interpolation, these ‘‘jaggy’’ artifacts may be enhanced too and affect the subsequent feature mapping process.

To reduce aliasing, we integrate prefiltering with interpolation. The interpolation process can be split into two steps. First, a continuous image  $I_C$  is reconstructed from the LR image  $I_L$  with an interpolation kernel  $r(x, y)$

$$I_C(x, y) = \sum_i \sum_j r(x-i, y-j) I_L(i, j) \quad (18)$$

where  $i$  and  $j$  are pixel indices in  $I_L$  varying inside the support region of  $r(x, y)$ .

Second, prefiltering is applied to clip the spectrum of  $I_C$ , attenuating the aliased frequency components. So  $I_C$  is convolved with a prefiltering kernel  $h(x, y)$ , and then sampled at the integer pixel to form a discrete image  $I_D^*$

$$I_D^*(i, j) = \iint h(i-x, j-y) I_C(x, y) dx dy \quad (19)$$

where  $i$  and  $j$  are pixel indices in  $I_D^*$  and the integral range is the support region of  $h(x, y)$ .

In the frequency domain, (18) and (19) equal to

$$F_D^*(\omega_x, \omega_y) = F_D(\omega_x, \omega_y) \cdot R(\omega_x, \omega_y) \cdot H(\omega_x, \omega_y) \quad (20)$$

where  $R(\omega_x, \omega_y)$  and  $H(\omega_x, \omega_y)$  are the Fourier transforms of  $r(x, y)$  and  $h(x, y)$ . The interpolation and prefiltering

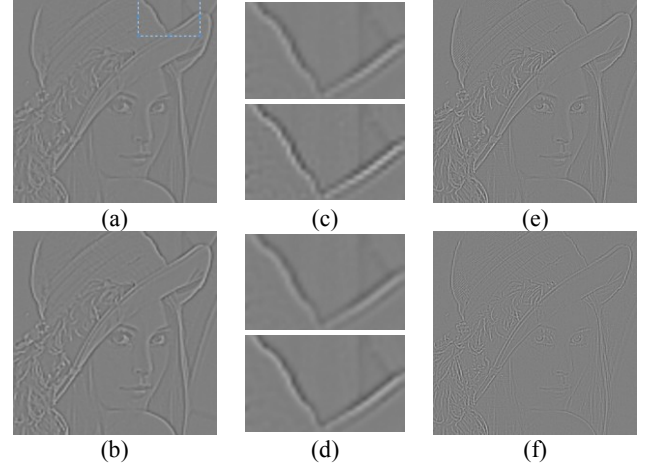


Figure 4: Feature information transfer. (a) LR features without feature enhancement; (b) LR features with feature enhancement; (c) top: close-view of (a), bottom: (a) with Richardson-Lucy deblurring [10]; (d) top: (a) with quadrature prefiltering [9], bottom: (a) with prefiltering and sparse prior deblurring [8]; (e) real missing HR features corresponding to (a); (f) real missing HR features corresponding to (b).

kernels are often selected as smoothing functions. This integration can effectively suppress the aliased frequency components while avoiding over-smoothing.

In practice, prefiltering is accomplished in the spatial domain. For a computational efficient antialiasing performance, we adopt the quadrature prefiltering method proposed in [9]. The integral in (19) is decomposed into a sum of integrals over  $M$  small fragments

$$I_D^*(i, j) = \sum_{m=1}^M e_m, \quad \text{where} \quad (21)$$

$$e_m = \iint_{R_m} h(x, y) I_C(i-x, j-y) dx dy$$

The partition of each integral range  $R_m$  is obtained along the direction with minimum intensity transition in a local region. Denote  $C_m$  the average value of  $I_C$  inside  $R_m$ , so

$$e_m = C_m \iint_{R_m} h(x, y) dx dy \quad (22)$$

Gaussian quadrature is then used to approximate the definite integral of the prefiltering kernel.

### 2.4. Feature information transfer

Since the interpolation with prefiltering effectively suppresses aliasing and the sparse prior deblurring produces sharp and noise-free edges, this combination avoids both over-smoothing and unwanted artifacts, and thus achieves a reliable feature enhancement performance. Figure 4 gives an example to illustrate the feature information transfer after feature enhancement. LR features in (a) are extracted from a bicubic interpolated image with a high-pass filter. (b) gives the result after feature enhancement. (c)

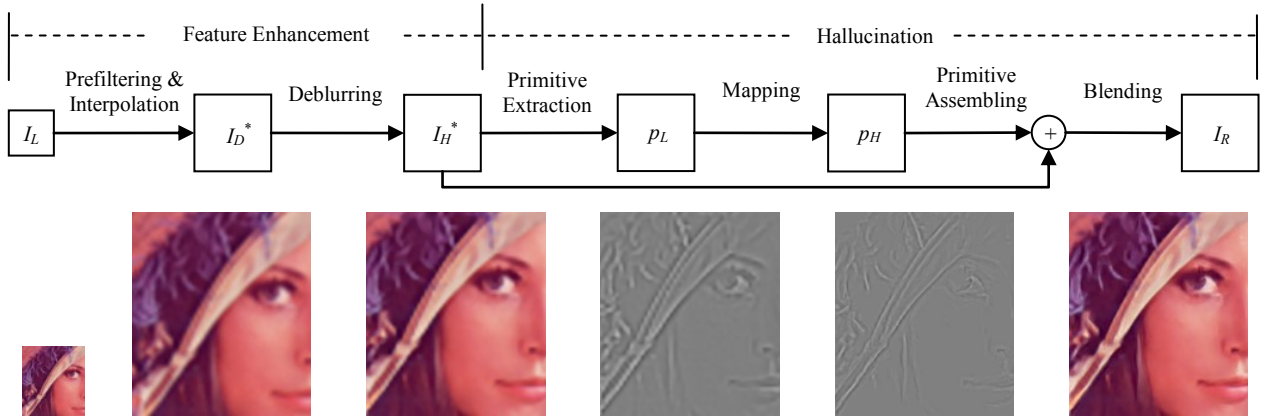


Figure 5: Framework of hallucination with feature enhancement

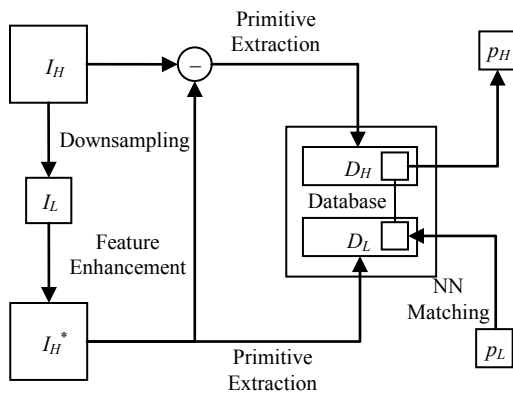


Figure 6: Learning and mapping

and (d) compare the enhanced LR features with Richardson-Lucy deblurring [10] and our method. It can be observed the jaggling artifacts exhibited in (c) are effectively alleviated in (d), whereas the edges still remain sharp. The real missing HR features in (a) and (b) are shown in (e) and (f), respectively. As the total feature energy is conserved, the contrast difference between (e) and (f), as well as (a) and (b), indicates the information transfer from HR features to LR ones. Consequently, the intrinsic dimensionality disparity between HR and LR features is reduced.

### 3. Image hallucination

#### 3.1. Framework

The framework of our hallucination scheme with feature enhancement is depicted in Figure 5. For an LR image  $I_L$ , an intermediate HR result  $I_D^*$  is first obtained through prefiltering integrated bicubic interpolation, where the prefiltering adopts a piecewise cubic filter kernel [11]. Then, sparse prior deblurring is performed on  $I_D^*$ , resulting in a feature enhanced image  $I_H^*$ . Features are extracted over the primitive manifold similar to that in [2], from  $9 \times 9$  image patches with a 6 pixel overlap in  $I_H^*$ . Each LR primitive



Figure 7: Training images ( $1536 \times 1024$  pixels).  $10^5$  pairs of primitive patches are extracted from these two images.

patch  $p_L$  is used to find a corresponding HR primitive patch  $p_H$  from prepared examples through feature mapping. Afterwards, the compatibility of neighboring HR primitives is enforced by averaging the feature values in overlapped regions. Finally, assembled HR primitives are added back to  $I_H^*$ , forming the hallucinated image  $I_R$ .

Figure 6 further illustrates the details of example learning and feature mapping. The learned knowledge exists in a database ( $D_L, D_H$ ) consisting of co-occurrence LR and HR primitive patches extracted from training images. For an input  $p_L$  in hallucination, we find its NN matching in  $D_L$  and use the corresponding patch in  $D_H$  as the output  $p_H$ .

The database used in our experiments is constructed from two representative natural images in Figure 7. A total of  $10^5$  primitive patch pairs are extracted from them. Note that the number of examples we used is much smaller than that required in [2]. However, we find this small database is sufficient for generic image hallucination with our feature enhancement, empirically. Methods adopting LLE [3] and CS [4] also use as small database as we do, but they often require within-category images in learning and mapping. Our proposed feature enhancement approach, differently, extends the ability of hallucination given content irrelevant training images.

#### 3.2. Feature mapping

With the reliably enhanced LR features, feature mapping can be improved in the sense that information to be learned is partially transferred to information acquired. To

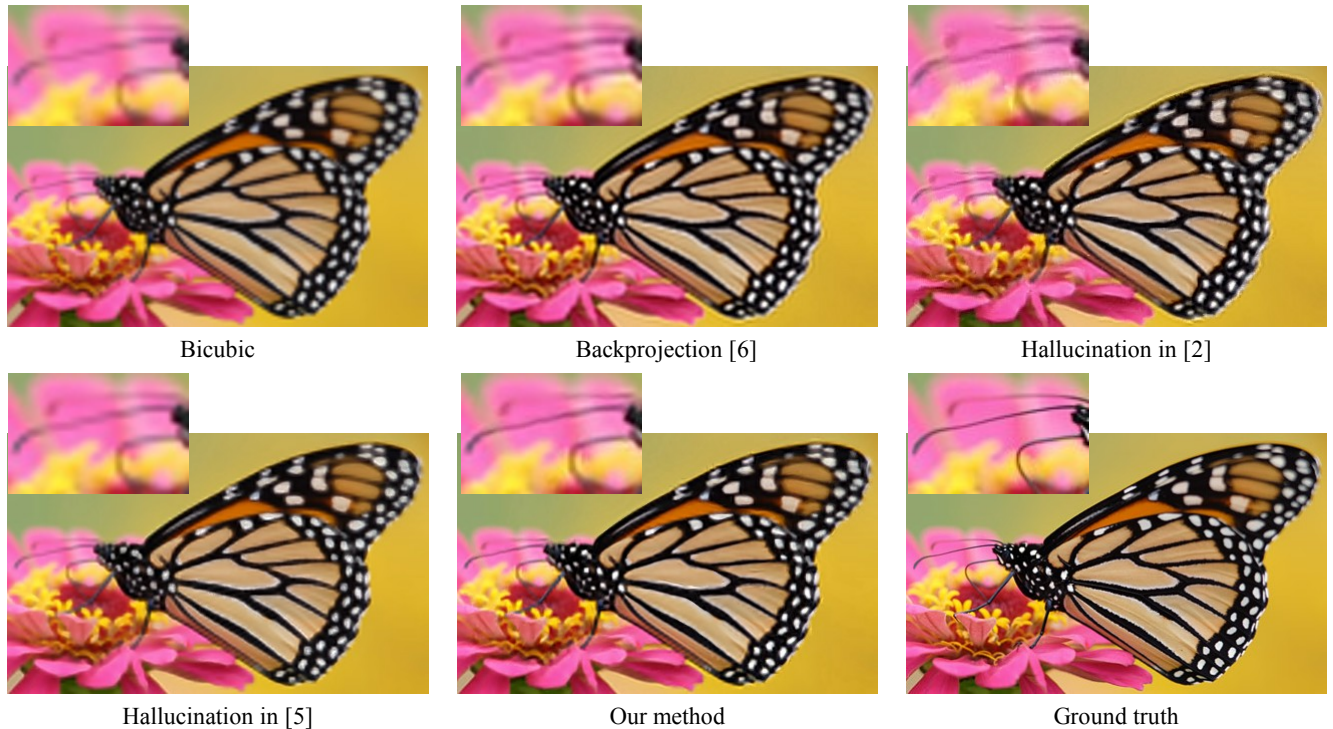


Figure 9: Comparison result of the “Monarch” image at 3× magnification

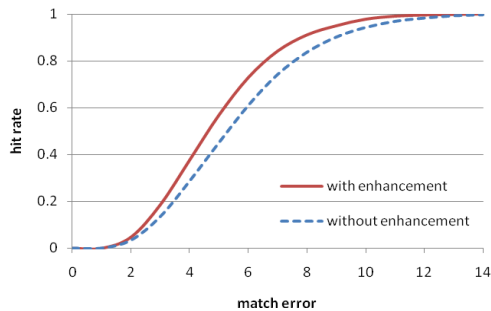


Figure 8: ROC curves of feature mapping accuracy over the primitive manifold, with and without feature enhancement.  $10^4$  primitive patches are tested over  $10^5$  trained examples.

evaluate the effect of feature enhancement in improving the feature mapping accuracy, we use the Receiver Operating Characteristic (ROC) curve to demonstrate the tradeoff between match error and hit rate. For a given match error  $e$ , the hit rate  $h$  is the percentage of test data whose match error is less than  $e$ . We define the match error as the RMS pixel error between the real missing HR primitive patch and that found through feature mapping (both are normalized by the contrast of the input LR primitive patch).

In Figure 8 two ROC curves are presented based on the feature mapping results of  $10^4$  primitive patches over  $10^5$  trained examples, with and without feature enhancement, respectively. The test data is sampled from images with irrelevant content to the training images. As can be ob-

served, the hit rate with feature enhancement is higher than that without feature enhancement at any match error, which indicates the proposed feature enhancement method steadily improves the feature mapping accuracy.

#### 4. Experiments

We test our hallucination scheme on a variety of color images with irrelevant content to the training images. In our experiment, original HR images are downsampled by Gaussian blurring with a standard variance of 1.4 followed by 1/3 decimation. In feature enhancement, the same Gaussian kernel is used for sparse prior deblurring (this additional information is not necessary, as deblurring with standard variance in a certain range give similar results). Since human observers are more sensitive to the luminance change in images, we only perform hallucination on the luminance component for color images.

Some experimental results are shown in Figures 9-11, all with a magnification factor of 3. Several typical single image super-resolution techniques; bicubic interpolation, backprojection [6] and previous hallucination [2, 5] are taken for comparison with the proposed approach. It can be observed that bicubic always gives the lowest quality results with blurring and jaggging artifacts along edges. Backprojection enhances the LR features to a certain extent, but meanwhile it introduces severe ringing artifacts during the iterative projection. Hallucination in [2] learns effective primal sketch priors from examples and produces

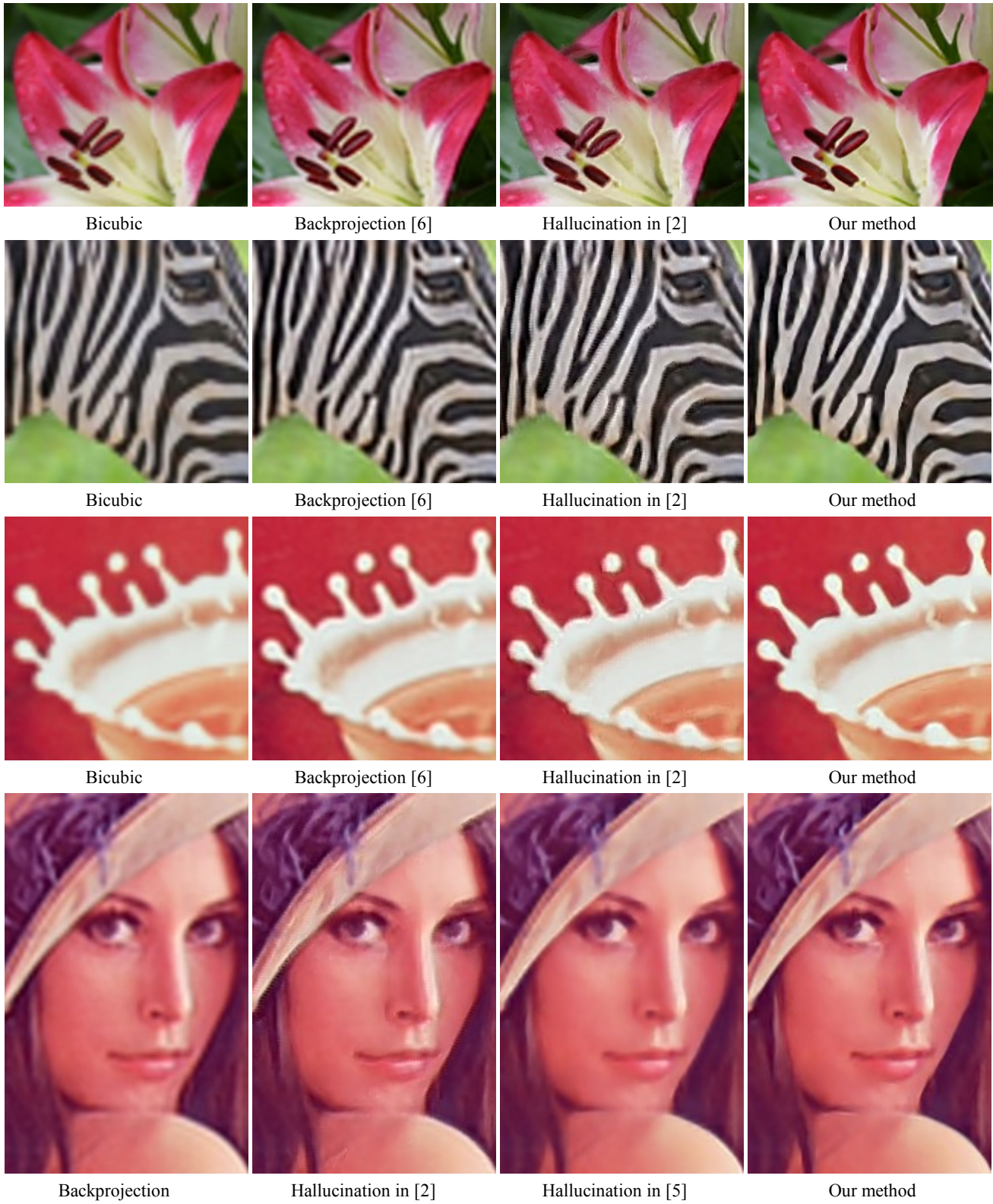


Figure 10: Comparison results of the “Lily”, “Zebra”, “Splash” and “Lena” images at  $3\times$  magnification

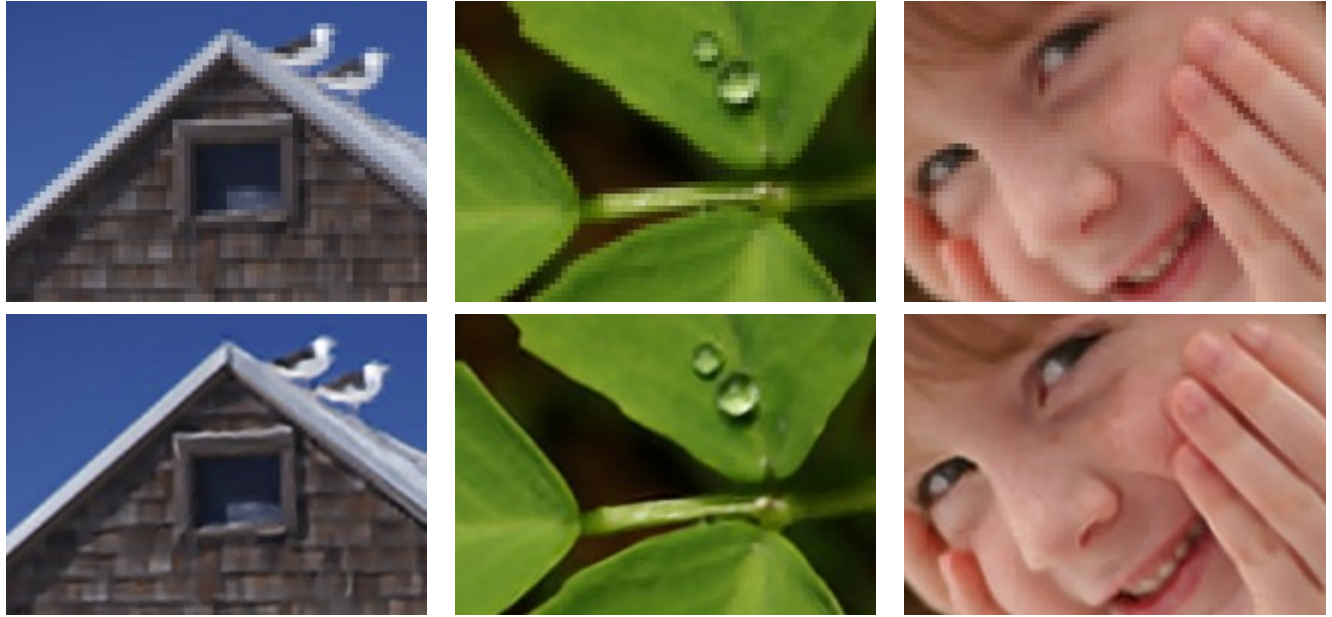


Figure 11: More results. Top: low-resolution inputs. Bottom: our hallucination results at  $3\times$  magnification.

Images	Bicubic	BP [6]	Hal [2]	Hal [5]	Ours
Monarch	14.99	13.08	13.08	12.49	<b>10.92</b>
Lily	8.75	8.17	8.32	7.78	<b>7.06</b>
Zebra	24.62	22.86	22.60	20.40	<b>19.57</b>
Splash	7.39	7.07	7.21	6.66	<b>6.50</b>
Lena	7.96	7.23	7.41	6.89	<b>6.49</b>

Table 1. RMS error of different super-resolution approaches

clearer edges than the above two approaches. However, due to inaccurate feature mapping, fine primitives are often not well recovered, leading to visible artifacts. Hallucination in [5] alleviates certain irregularities presented in [2] by introducing a two-phase feature mapping, whereas it rarely compensates the real missing information. In contrast, our approach reliably enhances the LR features and effectively suppresses different kinds of artifacts. Therefore, solid and clean edges are hallucinated, especially for fine primitives.

We also compare the above super-resolution approaches quantitatively in terms of the RMS error for the images in Figures 9 and 10. As shown in Table 1, our approach gives the most faithful super-resolution results to the original images. The run time of our algorithm is tested on a Pentium IV 3.0G PC, and it takes 60-100 seconds on average for an image with  $2\times 10^4$  pixels.

## 5. Conclusion

This paper proposes a feature enhancement method to improve the feature mapping accuracy in example-based super-resolution. Reliable feature enhancement is achieved through a combination of prefiltering integrated interpola-

tion and non-blind sparse prior deblurring, according to the analysis of feature information loss in downsampling. By redistributing feature information at different resolution levels, the feature mapping accuracy can be effectively improved. With a small number of examples, high quality images are hallucinated through our proposed approach.

## References

- [1] W. T. Freeman, E. C. Pasztor, and O. T. Carmichael. Learning low-level vision. *IJCV*, 2000.
- [2] J. Sun, N. Zheng, H. Tao, and H. Shum. Image hallucination with primal sketch priors. *CVPR*, 2003.
- [3] H. Chang, D. Yeung, and Y. Xiong. Super-resolution through neighbor embedding. *CVPR*, 2004.
- [4] J. Yang, J. Wright, Y. Ma, and T. Huang. Image super-resolution as sparse representation of raw image patches. *CVPR*, 2008.
- [5] L. Ma, Y. Zhang, Y. Lu, F. Wu, and D. Zhao. Three-tiered network model for image hallucination. *ICIP*, 2008.
- [6] M. Irani, and S. Peleg. Motion analysis for image enhancement: resolution, occlusion and transparency. *IJCVIP*, 1993.
- [7] B. A. Olshausen, and D. J. Field. Emergence of simple-cell receptive field properties by learning a sparse code for natural images. *Nature*, 1996.
- [8] A. Levin, and Y. Weiss. User assisted separation of reflections from a single image using a sparsity prior. *PAMI*, 2007.
- [9] B. Guenter, and J. Tumblin. Quadrature prefiltering for high quality antialiasing. *ACM Transaction on Graphics*, 1996.
- [10] L. Lucy. An iterative technique for the rectification of observed distributions. *Astronomical Journal*, 1974.
- [11] D. P. Mitchell, and A. N. Netravali. Reconstruction filters in computer graphics. *SIGGRAPH*, 1988.